

## X-ray absorption spectroscopy and magnetic circular x-ray dichroism in $\text{Ce}_2\text{Fe}_{17}\text{N}_3$

This article has been downloaded from IOPscience. Please scroll down to see the full text article.

1996 J. Phys.: Condens. Matter 8 2437

(<http://iopscience.iop.org/0953-8984/8/14/017>)

View [the table of contents for this issue](#), or go to the [journal homepage](#) for more

Download details:

IP Address: 171.66.16.208

The article was downloaded on 13/05/2010 at 16:29

Please note that [terms and conditions apply](#).

## X-ray absorption spectroscopy and magnetic circular x-ray dichroism in $\text{Ce}_2\text{Fe}_{17}\text{N}_3$

O Isnard<sup>†</sup>, S Miraglia<sup>†</sup>, D Fruchart<sup>†</sup>, C Giorgetti<sup>‡</sup>, E Dartyge<sup>‡</sup> and G Krill<sup>‡</sup>

<sup>†</sup> Laboratoire de Cristallographie, associé à l'Université Joseph Fourier, CNRS, BP 166, 38042 Grenoble Cédex 9, France

<sup>‡</sup> Laboratoire pour l'Utilisation du Rayonnement Electromagnétique, Bâtiment 209D, Université Paris Sud, 91405 Orsay, France

Received 19 September 1995, in final form 2 January 1996

**Abstract.** The effect of nitrogen insertion on the electronic properties of cerium and iron in  $\text{Ce}_2\text{Fe}_{17}$  has been studied by means of x-ray absorption spectroscopy (XAS) and magnetic circular x-ray dichroism (MCXD). The evolution of the electronic structure of cerium upon nitrogen insertion has been studied. It emerges from this MCXD study at the  $L_{2,3}$  edges of cerium that the cerium atoms bear a 5d magnetic moment of about  $0.4 \mu_B$  that is coupled antiferromagnetically to that of iron. The spin polarized EXAFS signal has been observed; an attempt to evidence the magnetic environment has been made in the light of previous neutron diffraction results. Comparison of EXAFS and spin polarized EXAFS is revealed to be an efficient new tool to distinguish between magnetic and non-magnetic atoms in the environment of the absorber. The analysis of the Fe K edge MCXD spectra shows that insertion of nitrogen induces a trend to strong ferromagnetism with an almost completely filled majority spin subband.

### 1. Introduction

Insertion of light interstitial elements such as H, C or N into the  $\text{R}_2\text{Fe}_{17}$  system (R = rare earth) has been found to modify their magnetic properties [1–5]. Spectacular increases of the magnetic ordering temperatures have been reported as well as changes of the magnetization behaviour. The most promising compounds are obtained with nitrogen insertion. From a technological point of view  $\text{Sm}_2\text{Fe}_{17}\text{N}_x$  is the best candidate and has been characterized for its structural and magnetic properties [6, 7]. This paper will be devoted to the effect of nitrogen insertion on the cerium-based compound  $\text{Ce}_2\text{Fe}_{17}$  studied by means of x-ray absorption spectroscopy (XAS) and magnetic circular x-ray dichroism (MCXD). The experiments reported hereafter are part of an ongoing study of the  $\text{R}_2\text{Fe}_{17}\text{X}_x$  system (R = rare earth, X = H, C or N) by means of XAS and MCXD.

The choice of cerium was first prompted by its ability to hybridize with the conduction electron, yielding the so-called intermediate valence state. The compounds  $\text{Ce}_2\text{Fe}_{17}$  and  $\text{Ce}_2\text{Fe}_{17}\text{N}_3$  have been also characterized by means of neutron diffraction and magnetization measurements. The drastic changes of the magnetic properties as well as the anomalous volume increase induced by light interstitial insertion in the  $\text{Ce}_2\text{Fe}_{17}$  system led us to suspect that cerium might undergo an electronic transition upon hydrogenation or nitrogenation.

A previous and similar study of the  $\text{Ce}_2\text{Fe}_{17}\text{H}_x$  [8] system has actually shown that the valence of cerium is moderately sensitive to the change of transition temperature and to the iron magnetization. In addition, it is worth noting that powder neutron diffraction

measurements did not reveal any ordered magnetic moment on cerium in any compound [2, 5]. At this stage, the question of subtle effects on cerium upon interstitial insertion as well as a study of the local magnetism of iron in this system was addressed.

In this respect XAS and MCXD experiments are particularly well suited.

Magnetic x-ray dichroism (MXD) is the magnetic field-induced polarization dependence of the absorption coefficient in the x-ray energy range. Depending on the character of the polarization [9], one distinguishes between linear (MLXD) [10] and magnetic circular (MCXD) x-ray dichroism. This latter magneto-optical effect has gained interest recently since it is now possible to obtain polarized light of high intensity over a broad spectral range in many synchrotron facilities. This technique is very appealing because, in addition to the element and orbital selectivity of XAS, recent calculations have yielded sum rules [11] which allow us to extract the orbital or spin contribution to the local moments.

In the phenomenological approach of MCXD, the one-electron model allows us to understand the physics of the phenomenon. Even though the conduction band which hosts the excited electron may be rather broad and the probed states are more or less localized, it is generally admitted that the level which hosts the excited electron is a spin detector and the MCXD experiments give the difference as a function of energy of the spin up and spin down occupation in the empty states.

## 2. Experimental details

The alloy was melted in a high-frequency induction furnace from very pure starting elements and then annealed at 1000 °C for about one week. Standard x-ray diffraction experiments revealed the samples to be single phase; the powder pattern was indexed using the hexagonal multiple cell. Nitrogenation was performed using the route developed in our laboratory and described elsewhere [5]. Details on the neutron diffraction experiments are reported in this reference. The Curie temperatures were determined using a Faraday-type torque balance. The magnetic measurements were carried out in the range 4.2–300 K using an axial extraction magnetometer operating in fields up to 7 T [12].

X-ray absorption spectra as well as MCXD spectra were recorded at LURE using a position sensitive detector in transmission mode at 0.3 mrad below the orbit plane (i.e. for about 80% right circularly polarized light). The procedure of data collection and the experimental set-up are described elsewhere [13, 14].

**Table 1.** Structural and magnetic data for Ce<sub>2</sub>Fe<sub>17</sub> and Ce<sub>2</sub>Fe<sub>17</sub>N<sub>3</sub>. The transition temperature (\*) of Ce<sub>2</sub>Fe<sub>17</sub> is a Néel temperature.

Compound	<i>a</i> (Å)	<i>c</i> (Å)	<i>V</i> (Å <sup>3</sup> )	<i>T<sub>c</sub></i> (K)	<i>M<sub>s</sub></i> (μ <sub>B</sub> /f.u.)
Ce <sub>2</sub> Fe <sub>17</sub>	8.489	12.413	774.8	225*	29.7
Ce <sub>2</sub> Fe <sub>17</sub> N <sub>3</sub>	8.739	12.738	842.5	728	37.7

## 3. Structural results

We have shown previously that the host R<sub>2</sub>Fe<sub>17</sub> structure is retained upon nitrogen insertion [5]. Nitrogen atoms are exclusively accommodated in available octahedral holes the coordination of which is 2 R atoms and 4 Fe atoms. A schematic representation of the

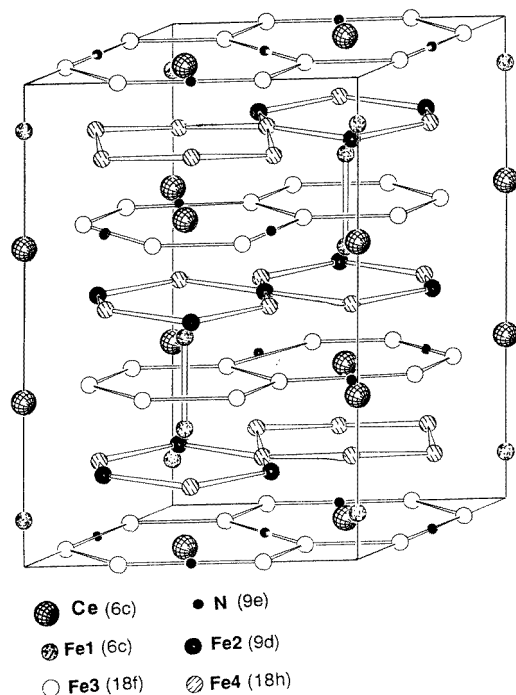


**Figure 1.** A schematic representation of the  $Ce_2Fe_{17}N_3$  structure.

**Table 2.** Distances relevant to cerium coordination in  $Ce_2Fe_{17}$  and  $Ce_2Fe_{17}N_3$ .

Atoms	$Ce_2Fe_{17}$	$Ce_2Fe_{17}N_3$
Ce–Fe(1) × 1	3.085	3.125
Ce–Fe(2) × 3	3.290	3.365
Ce–Fe(3) × 6	3.030	3.177
Ce–Fe(4) × 3	3.184	3.201
Ce–Fe(4) × 3	3.060	3.183
Ce–Fe(4) × 3	3.222	3.385
Ce–N × 3		2.525

crystal structure is given in figure 1. We here recall the main structural effects of nitrogen insertion:

- (i) an overall and mostly isotropic cell expansion (as can be seen from table 1) and
- (ii) an increase of particular Fe–Fe distances (dumbbell sites).

Another important effect regards the cerium coordination number, that is increased going from 19 in  $Ce_2Fe_{17}$  to 22 in  $Ce_2Fe_{17}N_3$ . The cerium coordination decomposes as follows: one Fe(1), three Fe(2), six Fe(3), nine Fe(4) and three additional N atoms in the case of the nitride (see [2] for the notation). We have reported in table 2 the distances relevant to the cerium coordination in  $Ce_2Fe_{17}$  and  $Ce_2Fe_{17}N_3$ . It can be seen that nitrogen insertion induces an average increase of the surrounding Ce–Fe distances that is about 0.11 Å. It is interesting to note that this effect is much more pronounced than for hydrogen insertion. Considering that the value of 0.11 Å is close to the difference in the radii of  $\gamma$ -Ce and  $\alpha$ -Ce

(1.824 and 1.73 Å respectively) [15], it is then reasonable to suspect that Ce has undergone an electronic transition from  $\alpha$ -Ce to  $\gamma$ -Ce upon nitrogen insertion. This consideration prompted the XAS experiments that are reported below.

#### 4. Magnetic results

Nitrogen insertion has drastic effects upon the magnetic properties of  $\text{Ce}_2\text{Fe}_{17}$ , the most spectacular being the increase of the transition temperature from 225 to 728 K, which is accompanied by a change of the magnetization behaviour; in this respect some useful parameters have been summarized in table 1. The increase of the magnetic ordering temperature has been already discussed widely in terms of enhancement of the exchange interaction and correlated with the observed release of the short Fe–Fe distances (so called dumbbells).

The saturation magnetization of  $\text{Ce}_2\text{Fe}_{17}$  and its corresponding nitride are given in table 1. The starting  $\text{Ce}_2\text{Fe}_{17}$  exhibits a helimagnetic structure below the Néel temperature of 225 K whereas  $\text{Ce}_2\text{Fe}_{17}\text{N}_3$  exhibits a ferromagnetic-like behaviour below the Curie temperature of 728 K.

The ferromagnetic structure of  $\text{Ce}_2\text{Fe}_{17}\text{N}_3$  was refined from neutron powder diffraction data, which showed that the local iron moments are increased upon nitrogeneration. The relative increase is almost 10% for most sites except on the 6c iron atoms (Wyckoff notation) for which the largest moment is observed with a relative 20% increase. It is also worth noticing that the neutron diffraction studies did not evidence a moment on the cerium sites. However this experimental fact does not rule out the eventuality of a weak and not localized or unordered moment on cerium. In this respect the MCXD experiments are particularly suitable to clarifying this point.

An additional reason for the MCXD experiments arose from crystal chemistry considerations which suggest Fe–N bonding to be predominant in the  $\text{R}_2\text{Fe}_{17}$  nitrides and likely to modify the local magnetism of iron. This assumption is supported by the fact that the strength of R–N bonds in  $\text{R}_2\text{Fe}_{17}\text{N}_3$  is weaker than that encountered in binary rare earth nitrides for a given coordination. It appears, instead, that Fe–N bonds are strong and comparable to those found in iron nitrides. It was thus suspected that, in this system, the iron moments might depend on the degree of 3d–2p hybridization with N atoms [16, 17].

Some hints at the magnetic properties of the iron 3d electrons can be found by studying the effect of pressure on the transition temperature. Using a picture in which nitrogen insertion may be regarded as a ‘negative chemical pressure’, the magnetic Grüneisen parameter can be derived and its dependence upon  $T_c$  then yields information on the itinerant or localized character of the 3d electrons. So far, no clear-cut conclusion could be drawn from such considerations rendering the MCXD study desirable.

#### 5. XAS experiments

As shown in the previous sections, the changes of the physical parameters induced by nitrogen insertion have a larger magnitude than those due to hydrogen insertion. In view of these considerations one could expect N insertion to have a larger effect on the cerium valence than has H insertion.

It is now rather well established [18, 19] that x-ray absorption measurements at the  $L_{2,3}$  edges of rare earth elements give a relevant representation of the electronic configuration and yield, especially for cerium compounds, the 4f occupation number. The determination

of the valence has been performed using a deconvolution technique from the mixed valent  $L_3$  spectra recorded at room temperature. All absorption spectra were normalized to the edge jump. The deconvolution process is based on a  $\tan^{-1}$  function which describes the transition from the 2p to the continuum states and Lorentzian functions that take into account both the 5d density of unoccupied states and the finite lifetime of the 2p core hole. The equation used is taken from Röhler [18]:

$$\begin{aligned}
 F(E) = B_0 + B_1E + S \left\{ \left( (\Delta E/2) A_k \sum_{i=0,9} f_i \right) / (E - (E_k - i\varepsilon_k))^2 + (\Delta E/2)^2 \right. \\
 + \left( (\Delta E/2) A_l \sum_{i=0,9} f_i \right) / (E - (E_l - i\varepsilon_l))^2 + (\Delta E/2)^2 \\
 + \frac{A_k \varepsilon_k}{(A_k \varepsilon_k + A_l \varepsilon_l)} \left[ \frac{1}{2} + \frac{1}{\pi} \tan^{-1} \left( \frac{(E - (E_k + \delta))}{(\Delta E/2)} \right) \right] \\
 \left. + \left( 1 - \frac{A_k \varepsilon_k}{(A_k \varepsilon_k + A_l \varepsilon_l)} \right) \left[ \frac{1}{2} + \frac{1}{\pi} \tan^{-1} \left( \frac{(E - (E_l + \delta))}{(\Delta E/2)} \right) \right] \right\}
 \end{aligned}$$

where  $B_1$  and  $B_0$  describe the linear background parameters,  $S$  is the scale factor; the first accessible 5d states in  $4f^{n+1}$  and  $4f^n$  configurations are denoted by  $E_k$  and  $E_l$  respectively. The two lines of empty 5d states are represented by 10 values assumed to be equally spaced in energy; the spacings  $\varepsilon_k$  and  $\varepsilon_l$  are allowed to be different for the two white lines. Finally  $\Delta E$  is the core hole lifetime and  $A_k$  and  $A_l$  are factors of the amplitudes.

The non-integral occupation of the 4f shell,  $n_f$  (or the valence  $v = 4 - n_f$ ) can be easily deduced using a least-squares fitting procedure. In  $Ce_2Fe_{17}$ , the cerium atoms are known to be in an intermediate valence state of 3.33. A study of the  $Ce_2Fe_{17}N_3$  x-ray absorption near-edge structure (XANES) reveals a two-bump structure associated with  $4f^1$  and  $4f^0$  channels in the final state. The presence of both  $4f^1$  and  $4f^0$  configurations bears witness to the persistence of a mixed valence state after nitrogen insertion. The XAS spectra show that an  $\alpha$ -Ce-to- $\gamma$ -Ce-like transition does not occur. A slight decrease of the Ce valence from  $v = 3.33$  in  $Ce_2Fe_{17}$  to  $v = 3.307$  for  $Ce_2Fe_{17}N_3$  is nevertheless observed and may indicate a small reduction of 5d-4f hybridization. As shown in figure 2 the change we observe in the case of  $Ce_2Fe_{17}N_3$  is only 15% of that observed in  $Ce_2Fe_{17}H_5$ . Thus, in spite of larger effects on the magnetic properties, nitrogen insertion leads to a weaker evolution of the cerium valence than hydrogen does. In this respect a relevant comparison can be made between the compounds  $Ce_2Fe_{17}H_3$  and  $Ce_2Fe_{17}N_3$ , which are fully isostructural, that is the interstitial atoms N and H occupy the same sites. This shows that H and N do not behave in the same way in the  $Ce_2Fe_{17}$  crystal structure. As already discussed, it is known that Fe-H bonding is much weaker than Fe-N bonding; since N participates more strongly in bonding with Fe than does H, it can be surmised that R-H and R-N bonding will differ. This also stresses the fact that the magnetism of iron seems to be more sensitive to interstitial insertion than cerium is and, presumably, governs the physical properties of these compounds as discussed in the previous sections.

## 6. MCXD experiments

MCXD on delocalized systems was first observed by Schutz *et al* [20] on Fe K edge, although predicted 21 years ago by Erskine and Stern [21]. The understanding of this phenomenon is being nowadays improved because of the large amount of theoretical as well as experimental work in this new spectroscopic area. In the case of delocalized systems,

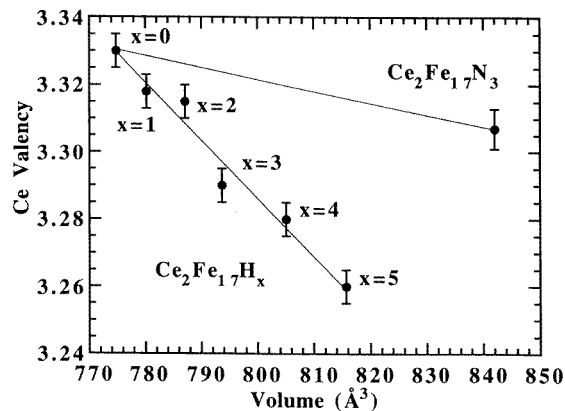


**Figure 2.** Evolution of the cerium valency upon interstitial insertion as a function of interstitial concentration. The data for Ce<sub>2</sub>Fe<sub>17</sub>H<sub>x</sub> are taken from [8].

as mentioned above the approach is rather phenomenological [20]. Jo and Imada [22] have developed a model which takes into account the inter-band interaction, whereas according to Harmon *et al* [23, 24], in the description of the MCXD at the L edges of rare earths, the overlapping of the radial part of the wave function of the core hole (2p) and that of the 5d electrons depends on the 5d spin and cannot be neglected. More MCXD experimental results are needed to refine the validity of these models. It is one of the purposes of this study to contribute to a quantitative description of the MCXD signal and to improve the understanding of the electronic structure of cerium in highly correlated systems. What is important for our purpose here is to remember that in the  $\alpha$ -Ce compound MCXD signals at the L<sub>2,3</sub> absorption edges of the rare earth can be interpreted as those of a 5d system without a 4f electron (e.g. LuFe<sub>2</sub>). Finally, work has recently been carried out to probe the possibility of quadrupole transitions [24–26].

## 7. MCXD at the Ce L<sub>2</sub> and L<sub>3</sub> edges

Because of the high Curie temperature of Ce<sub>2</sub>Fe<sub>17</sub>N<sub>3</sub> (728 K), room-temperature MCXD measurements yield the total saturated moment ( $T/T_c \approx 0.4$ ). Some measurements made at low temperature confirm this point. The difference in  $M_s$  between 4.2 K and room temperature is 4%; this should not significantly affect the signal.

We use exactly the same procedure as described in [8] to analyse the shape, amplitude and sign of the MCXD signal at the Ce L<sub>2,3</sub> edges. Because of the electric dipole selection rules the probed states are the 5d ones, and the MCXD signal gives a fingerprint of the 5d moment on Ce. The fact that we observed the double structure in the MCXD is characteristic of a mixed valence state since two possible screening mechanisms of the 2p core hole are induced by the strong hybridization between the 4f state and the conduction band.

We have made an estimation of the magnitude of this 5d moment by scaling the normalized area of the dichroic signal to that of previously well characterized compounds such as CeFe<sub>2</sub> or LuFe<sub>2</sub>, compounds where the 5d moment has been determined independently by band structure calculation and polarized neutron diffraction experiments. The estimated value from the observed intensity of the MCXD signal is  $-0.4 \mu_B$ , which lies very close to that estimated for the hydrogenated compounds [8]. The error bar can

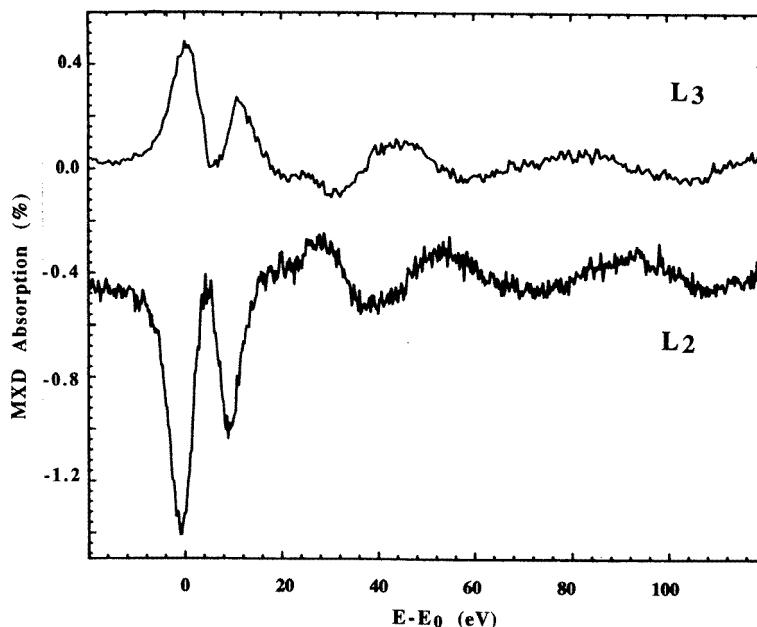
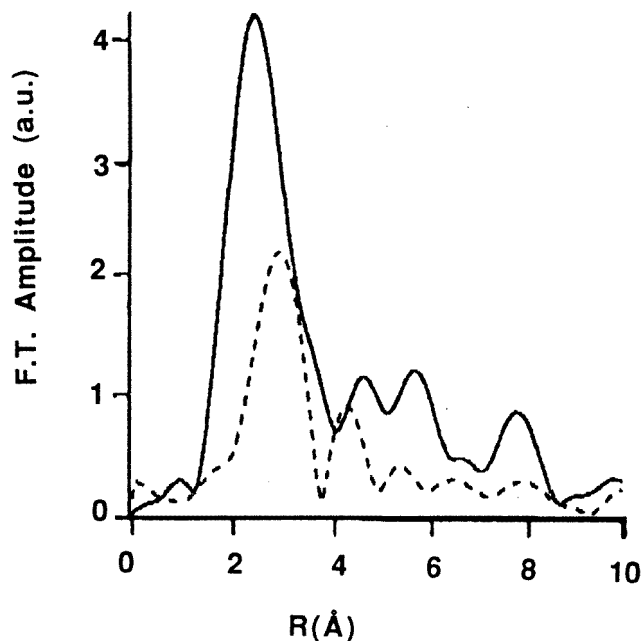


Figure 3. The room-temperature MCXD signal at the Ce  $L_{2,3}$  edges for  $Ce_2Fe_{17}N_3$ .

be estimated as  $0.05\text{--}0.1 \mu_B$ . Furthermore this value is very close to that predicted by band structure calculations for the  $Y_2Fe_{17}N_3$  compound [27,28]. As shown in figure 3, the branching ratio between the dichroic signal at  $L_2$  and  $L_3$  edges is exactly  $-2$ . In other words, it has been shown that the difference of the integrated absorption intensity for circularly polarized light parallel ( $I^+$ ) and antiparallel ( $I^-$ ) to the magnetization direction is proportional to the ground state expectation value of the orbital moment  $\langle L_z \rangle$  per hole. The MCXD spectra recorded at the  $L_{2,3}$  edges and normalized by the edge of the unpolarized absorption edge have been plotted in figure 3. The use of the first sum rule leads to a zero value for  $\langle L_z \rangle$  since the integrated intensity of the MCXD signal at the  $L_2$  edge is opposite to that of the  $L_3$  edge. This clearly shows that the 5d magnetic moment is only from spin origin in the ground state. Finally it should be noticed that for a fully trivalent state of cerium this branching ratio has been shown to significantly depart from  $-2$ . The observance of this  $-2$  branching ratio is thus a clear evidence that the 4f electrons are strongly hybridized with the 5d–3d conduction electrons.

As can be seen in figure 4, comparison of the EXAFS signal with the spin polarized EXAFS (SPEXAFS) reveals a significant difference between the magnetic and non-magnetic environments. Owing to the crystal structure determination from neutron diffraction experiment, we can describe the first peak of the EXAFS signal Fourier transform as being due to the contribution of both the three nitrogen atoms at  $2.5 \text{ \AA}$  from cerium and the 13 iron atoms at about  $3.2 \text{ \AA}$ ; an additional shell of six iron neighbours is present at about  $3.4 \text{ \AA}$ . Whereas the Fourier transform of the EXAFS signal exhibits the contribution of the two kinds of neighbour, the SPEXAFS signal shows the contribution of the iron atoms only. The lack of a complete theoretical description of the SPEXAFS signal prevents us from a further quantitative analysis of the distances and of the number of magnetic and non-magnetic species.





**Figure 4.** Fourier transforms (FTs) of the EXAFS and SPEXAFS signals at the  $L_2$  edge of cerium in arbitrary units. The dotted line refers to the SPEXAFS signal magnified by 100, and the solid line represents the EXAFS Fourier transform.

### 8. MCXD at the Fe edge

By studying several 3d–3d and 3d–4f systems at the K edge of the 3d element, Stähler *et al* [29] have demonstrated that there is no proportionality between the calculated p or d orbital moment on Fe and the area of the MCXD signal. Nevertheless, the analysis of the shape of the MCXD signal at the K edge of iron is of great interest. A two-sharp-peak structure is observed for both compounds,  $Ce_2Fe_{17}$  and  $Ce_2Fe_{17}N_3$ . As in a previous study we have been interested in correlating the evolution of the intensity of the low-energy peak with the filling of the majority 3d band [8]. This relation is based on the fact that elemental iron exhibits a two-peak structure whereas well known strong ferromagnetic materials such as Ni or Co display a single-peak structure [30]. We rely on recent studies of Co–Fe multilayers which show a weakening of the intensity of the low-energy peak when the Co concentration increases accordingly [28, 31, 32]. According to these studies the shape and amplitude of the dichroic signal at the K edge of iron reflect the filling scheme of the 3d subbands. Considering this experimental fact, we ascribe the slight decrease of this first peak to a trend to strong ferromagnetism. This assumption is supported by band structure calculations that were made on the isotypical  $Y_2Fe_{17}N_3$  compound [27, 28, 33]. These calculations predict a filling of the majority 3d band upon nitrogen insertion. As mentioned earlier, we think that in  $Ce_2Fe_{17}N_3$  a strong Fe(3d)–N(2p) hybridization is present and that it gives way to charge transfers. It is seen from figure 5 that  $Ce_2Fe_{17}N_3$  and  $Ce_2Fe_{17}H_5$  exhibit similar MCXD spectra despite their very different interstitial concentrations. One can conclude that the influence of nitrogen insertion upon the Fe 3d band structure is found to be much stronger than that of hydrogen. A narrowing of the iron 3d band cannot be excluded since studies

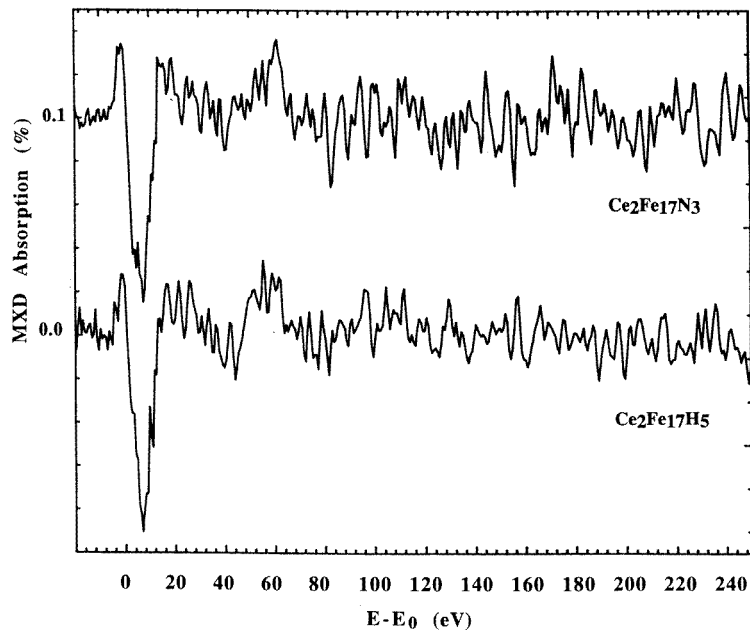


**Figure 5.** A comparison of the MCXD signals at the Fe K edge for  $Ce_2Fe_{17}H_5$  and  $Ce_2Fe_{17}N_3$ .

of volume effects in  $R_2Fe_{17}C_x$  compounds have shown, for the iron magnetism, a gradual transition from an itinerant behaviour in  $R_2Fe_{17}$  to a rather localized one in  $R_2Fe_{17}C_x$  [34].

A comparison of the MCXD signals at the Ce  $L_{2,3}$  and Fe K edges reveals that, in  $Ce_2Fe_{17}N_3$ , the Ce 5d magnetic moment is coupled antiparallel to the Fe 3d magnetic moment. Such a coupling is in agreement with previous results on  $CeCo_5$ ,  $CeFe_2$  and  $Ce_2Fe_{17}H_x$  compounds [14, 18].

Finally, a careful look at figure 5 shows that both  $Ce_2Fe_{17}N_3$  and  $Ce_2Fe_{17}H_5$  exhibit a positive peak at about 60 eV after the Fe absorption K edge. Such a phenomenon has been observed previously in pure  $\alpha$ -iron and has been ascribed to multielectronic excitation [35]. Despite the small MCXD signal at the iron K edge, the observance of the even weaker multielectron excitation bears witness to the quality of the spectra.

## 9. Conclusion

This spectroscopy study has mainly shown that the valence of cerium in  $Ce_2Fe_{17}$  is less affected upon nitrogen insertion than hydrogen insertion. An interesting result is that the contribution to magnetism of cerium atoms is of 5d character (spin only). Another remarkable feature is that the magnetism of these compounds is governed by the changes of the iron magnetism. We have no evidence for a localized contribution to magnetism of 4f origin. There is still an open question regarding the origin of the persistence of a mixed valent state in cerium upon interstitial insertion. We recall that in  $CeFe_2$ , where interstitial insertion leads to a localization of the 4f states of cerium, an amorphization takes place upon hydrogen insertion and then the local environment of cerium is no longer preserved. In addition, considering that similar effects seem to take place in  $Ce_2Fe_{17}$  and  $Ce_2Fe_{14}B$  systems where the rare earth coordinations are comparable (CN = 20 in  $Ce_2Fe_{14}B$  and CN = 19 in  $Ce_2Fe_{17}$ ) and iron rich, we think that steric considerations could be part of the

answer. The 5d moment that has been evidenced by MCXD however is roughly of the same magnitude whatever the inserted element. This means that interstitial insertion does not induce significant charge transfers towards the 5d band of cerium. We have shown that the local magnetism of iron is affected upon nitrogen insertion, and we have observed a qualitative evidence for a strong ferromagnetic-like behaviour of iron in this system.

## References

- [1] Zhong X P, Radwanski R J, de Boer F R, Jacobs T H and Buschow K H J 1990 *J. Magn. Magn. Mater.* **86** 333–40
- [2] Isnard O, Miraglia S, Soubeyrou J L, Fruchart D and Stergiou A 1990 *J. Less-Common Met.* **162** 273–84
- [3] Coey J M D, Lawler J F, Sun H and Allan J E M 1991 *J. Appl. Phys.* **69** 3007
- [4] Buschow K H J 1991 *NATO ASI series C* vol 331, ed G J Long and F Grandjean (Dordrecht: Kluwer) pp 527–52
- [5] Isnard O, Miraglia S, Soubeyrou J L and Fruchart D 1992 *J. Alloys Compounds* **190** 129–35
- [6] Isnard O, Miraglia S, Kolbeck C, Tomey E, Soubeyrou J L, Fruchart D, Guillot M and Rillo C 1992 *J. Alloys Compounds* **178** 15–22
- [7] Isnard O, Miraglia S, Guillot M and Fruchart D 1994 *J. Appl. Phys.* **10** 5988–93
- [8] Isnard O, Miraglia S, Fruchart D, Giorgetti C, Pizzini S, Dartyge E, Krill G and Kappler J P 1994 *Phys. Rev. B* **49** 15 692
- [9] Dartyge E, Fontaine A, Baudelet F, Giorgetti C, Pizzini S and Tolentino H 1992 *J. Physique I* **2** 1233–55
- [10] Van der Laan G, Thole B T, Sawatsky G A, Goedkoop J B, Fuggle J C, Esteva J M, Karnatak R, Remeika J P and Dabkowska H A 1986 *Phys. Rev. B* **34** 6529
- [11] Carra P, Thole B T, Altarelli M and Wang X 1993 *Phys. Rev. Lett.* **70** 694
- [12] Isnard O, Miraglia S, Fruchart D, Deportes J and L'Heritier P 1994 *J. Magn. Magn. Mater.* **131** 76–82
- [13] Fontaine A, Dartyge E, Itié J P, Jucha A, Polian A, Tolentino H and Tourillon G 1989 *Topics in Current Chemistry* vol 151, ed E Hasnain (Berlin: Springer) pp 179–203
- [14] Giorgetti C, Pizzini S, Dartyge E, Fontaine A, Baudelet F, Brouder C, Krill G, Miraglia S, Fruchart D and Kappler J P 1993 *Phys. Rev. B* **48** 12 732
- [15] Gschneidner K A and Smoluchowski R 1963 *J. Less-Common Met.* **5** 374
- [16] Isnard O 1993 *PhD Thesis* University of Grenoble
- [17] Isnard O and Fruchart D 1994 *J. Alloys Compounds* **205** 1–15
- [18] Röhler J 1985 *J. Magn. Magn. Mater.* **47–48** 175–80
- [19] Röhler J 1987 *Handbook on the Physics and Chemistry of Rare-earths* vol 10, ed K A Gschneidner, J R Eyring and S Hufner (Amsterdam: North-Holland) pp 453–544
- [20] Schutz G, Wagner W, Wilhelm W, Kielne P, Zeller R, Frahm R and Materlik G 1987 *Phys. Rev. Lett.* **58** 737–40
- [21] Erskine J L and Stern A 1975 *Phys. Rev. B* **12** 5016
- [22] Jo T and Imada S 1994 *J. Phys. Soc. Japan* **62** 3721
- [23] Harmon B N and Freeman A J 1974 *Phys. Rev. B* **10** 1979
- [24] Lang J C, Srajer G, Detlefs C, Goldman A I, König H, Wang X, Harmon B N and McCallum R C 1995 *Phys. Rev. Lett.* **74** 4935
- [25] Giorgetti C, Dartyge E, Brouder C, Baudelet F, Meyer C, Pizzini S, Fontaine A and Galéra R M 1995 *Phys. Rev. Lett.* **75** 3186
- [26] Wang X, Leung T C, Harmon B N and Carra P 1993 *Phys. Rev. B* **47** 9087
- [27] Jaswal S S 1992 *IEEE Trans. Magn.* **MAG-28** 2322–5
- [28] Jaswal S S 1995 *NATO Conf. on Interstitial Alloys for Reduced Energy Consumption and Pollution (Il Ciocco, 1994)* ed F Grandjean, G J Long and K H J Buschow (New York: Plenum) p 411
- [29] Stähler S, Schütz G and Ebert H 1993 *Phys. Rev. B* **47** 818–26
- [30] Giorgetti C 1994 *PhD Thesis* University of Orsay
- [31] Pizzini S, Fontaine A, Dartyge E, Giorgetti C, Baudelet F, Kappler J P, Boher P and Giron F 1994 *Phys. Rev. B* **50** 3779
- [32] Hikam M 1992 *PhD Thesis* University of Nancy
- [33] Li Y P, Li H-S and Coey J M D 1991 *Phys. Status Solidi b* **166** K107–12
- [34] Valeanu M, Plugaru N and Burzo E 1994 *Phys. Status Solidi* **184** K77–80
- [35] Dartyge E, Baudelet F, Brouder C, Fontaine A, Giorgetti C, Kappler J P, Krill G, Lopez M F and Pizzini S 1995 *Physica B* **208 & 209** 751–4